# Validation of Significant Wave Height From Improved Satellite Altimetry in the German Bight

Marcello Passaro, *Student Member, IEEE*, Luciana Fenoglio-Marc, *Member, IEEE*, and Paolo Cipollini, *Senior Member, IEEE*

***Abstract*—Significant wave height (SWH) is mapped globally through satellite altimetry. SWH estimation is possible because the shape of a pulse-limited altimetric waveform depends on the sea state. The algorithm for SWH also depends on the width of the point target response (PTR) function. Particularly challenging for SWH detection are coastal data, due to land and calm water interference in the altimeter footprint, and low sea states, due to an extremely sharp leading edge in the waveform that is consequently poorly sampled. Here, Adaptive Leading Edge Subwaveform Retracker (ALES), a new algorithm for reprocessing altimetric waveforms, will be validated for SWH estimation in the German Bight. This challenging region presents both low sea state and coastal issues, and an extended network of buoys of the Bundesamt fuer Seeschiffahrt und Hydrographie is available for the *in situ* validation. Reprocessed data from Envisat, Jason-1, and Jason-2 missions are validated against the three offshore buoys. The *in situ* validation is applied both at the point nearest to the buoy and at all other points along track. The skill metrics is based on bias, standard deviation, slope of regression line, and number of cycles with correlation larger than 90%. We also tested the impact of the inclusion of two additional waveform samples that are provided in the Envisat Sensor Geophysical Data Records and the adoption of different values for the width of the PTR. Results show that near coast ALES estimations of SWH are generally better correlated with buoy data than standard processed products.**

***Index Terms*—Buoy, coastal altimetry, German bight, retracking, satellite altimetry, significant wave height (SWH), subwaveform retracker, tidal flats, validation.**

## I. Introduction

OCEAN waves are a fundamental expression of the air–sea interaction which is of major importance for climate research, but they also greatly impact a broad range of economic and engineering activities. The design, planning, and successful operation of these activities rely on an accurate description of the sea state.

*In situ* wave observations are obtained from buoys and voluntary observing ships (VOSs). VOS data are geographically limited to the commercial routes and absent for high sea states, when vessels avoid the navigation, while buoys provide a reliable source for the calibration and validation of other sensors but are limited by the high cost and are hardly suitable even to a basin scale study [1].

Waves are also measured remotely, most importantly by spaceborne synthetic aperture radar (SAR) and radar altimeters. Algorithms have been designed and calibrated to extract integral wave parameters from a SAR image and even to derive a 2-D ocean wave spectrum [2]. For satellite altimetry, which is the focus of this study, the determination of significant wave height (SWH) over the open ocean is a mature procedure, which has yielded over two decades of global and repeated measurements along the tracks of several satellites. SWH is defined to be the average crest-to-trough height of the 1/3 highest waves and is usually considered to be equivalent to four times the standard deviation (std) of the wave height distribution [3].

Wave forecasts are, of course, particularly important for operational purposes, and remotely sensed SWH can be used for validation purposes [4], while data assimilation can have a significantly positive impact on model performances [5]. Models are nevertheless less effective in the coastal zone and, in general, in shallow water areas, where wave length and wave height vary depending on the depth (shoaling effect) and the interaction with the bottom causes wave energy dissipation into turbulence (radiation stress) [2]. SWH from satellite altimetry could play a key role in describing the wave conditions in these challenging areas, but altimetry encounters limitations in coastal areas that call for specialized processing.

To understand these limitations, it is necessary to focus on how a radar altimeter works. In all the conventional pulse-limited altimetry missions, a short pulse of radiation with known power is transmitted from a satellite toward the sea.[1] The pulse interacts with the rough sea surface, and part of the incident radiation within the altimetric footprint reflects back to the radar altimeter, which records the returned echo of the pulse.

Manuscript received April 16, 2014; revised June 25, 2014; accepted August 28, 2014. The first author is grateful to Prof. Dr.-Ing. Matthias Becker and to the Deutsche Forschungsgemeinschaft (Project COSELE) for the support during the stay at the Institute for Physical and Satellite Geodesy (PSGD) in Darmstadt. This work was supported in part by the ESA/DUE eSurge (ESA/ESRIN Contract 4000103880/11/I-LG) project.

M. Passaro is with the Graduate School, National Oceanography Centre Southampton (GSNOCS), University of Southampton, Southampton SO14 3ZH, U.K. (e-mail: marcello.passaro@noc.soton.ac.uk).

L. Fenoglio-Marc is with the Institute of Physical Geodesy, Technische Universität Darmstadt, 64287 Darmstadt, Germany.

P. Cipollini is with the Marine Physics and Ocean Climate Research Group, National Oceanography Centre, Southampton SO14 3ZH, U.K.

Color versions of one or more of the figures in this paper are available online at http://ieeexplore.ieee.org.

Digital Object Identifier 10.1109/TGRS.2014.2356331

[1] In reality, a long frequency-modulated chirp pulse is used for technical reasons. This is demodulated (deramped) after reception so that the measurement process can be effectively described as the interaction of a short pulse with the sea surface.

The power of the signal as received by the satellite is registered in a time series called a "waveform," and its resolution cell is called a "gate." Each individual echo is strongly perturbed by Rayleigh noise (speckle) coming from the incoherent addition of signals from reflecting facets inside the satellite footprint [6]. In order to limit this noise, typical downlinked "high-rate" waveforms at ∼20 Hz (one measurement every ∼300 m) are an average of 100 consecutive samples. Each high-rate waveform is fitted to a modeled echo in order to extract the parameters of interest in a process called "retracking".

In the open ocean, the vast majority of waveforms present a fast rising leading edge and a slowly decaying trailing edge and are well modeled by the Brown functional form [7], [8]. Any residual noise, particularly evident along the trailing edge, can influence the correct retrieval of the parameters of interest. This happens particularly in the last 0–20 km from the coastline: in this coastal strip, both calm highly reflective sheltered waters and raised land can contribute anomalous (i.e., non-Brown) returns within the altimeter range window, changing the waveform shape from that expected for a homogeneous surface [9].

To overtake this limitation, the Adaptive Leading Edge Subwaveform Retracker (ALES) has been designed to fit the Brown functional form to only a portion of the waveform which includes the leading edge. The width of this subwaveform is set depending on the SWH in order to maintain the same degree of precision both in open ocean and along the coast. The sea surface height estimation from ALES has already been validated and results have shown the improvements that this strategy can bring in challenging coastal areas [10]. The aim of this paper is to demonstrate that ALES performs better than the standard retrackers also for the SWH estimation from Envisat, Jason-2, and Jason-1 satellite altimetry missions.

This validation exercise is performed by comparing SWH from retracked altimetry data with *in situ* observations from buoys located in the German Bight (North Sea), which have already been compared with wave model outputs in [11] and with model and altimeter data in [12]. The area is a particularly challenging test bed for satellite altimetry: It is dominated by tides ranging from 2 to 4 m and characterized by shallow water and large exposed tidal flats during low tide [13]. Other peculiar targets in the area are patches of still water in the tidal flats and the land of the numerous islets, both impacting the radar return when they enter the satellite footprint.

Section II describes the way that SWH is estimated in ALES, the main issues that characterize the retrieval process, and the methodology used for validating the results. In Section III, the data sets from satellite altimetry and *in situ* buoys are presented. Section IV evaluates different retracking choices made for Envisat, presents in detail the results of the validation, and discusses the findings. Section V summarizes the conclusions of this paper.

## II. Methods

### A. Estimation of SWH

ALES adopts the Brown theoretical ocean model and fits it to each high-rate waveform through an unweighted least square

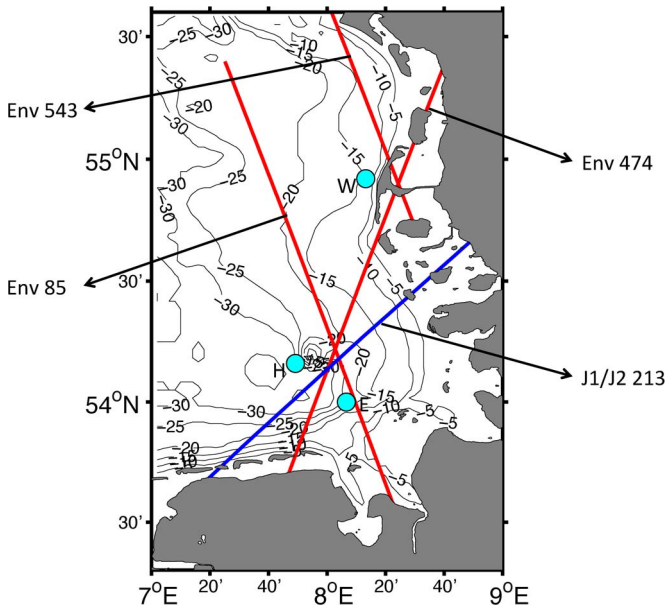


Fig. 1. Areas of study and the extent of the retracked altimetry passes. Bathymetry is shown by means of contour lines: They are drawn every 5 m.

estimator. A complete physical description of the functional form is given in [7] and [10].

The parameters which are estimated by ALES are three: the Epoch $\tau$, i.e., the position of the midpoint of the leading edge with respect to the fixed nominal tracking point determined by the onboard tracker (related to the sea surface height); the rise time of the leading edge, which is related to the SWH; the amplitude of the received signal, from which the backscatter coefficient $\sigma^0$ is derived and then related to the wind speed. For a graphical description of the parameters to be estimated on an idealized waveform without noise, the reader can refer to [10, Fig. 1].

The rise time of the leading edge $(\sigma_c)$ depends on the width of the radar point target response (PTR) $\sigma_p$ and on a term $\sigma_s$ linked to SWH by the following equation:

$$\sigma_c^2 = \sigma_p^2 + \sigma_s^2 \qquad \sigma_s = \frac{SWH}{2c} \tag{1}$$

where c is the speed of light. It is important here to stress the meaning of $\sigma_p$. The PTR convolved with the probability density function of the sea surface height distribution and the step function defines the average of the illuminated area within the satellite footprint [3]. The PTR has the form of a $sinc^2$ function and, in order to simplify the convolution, is approximated in the Brown model by a Gaussian function of which $\sigma_p$ describes the width

$$PTR(t) \approx \exp\left(\frac{-t^2}{2\sigma_p^2}\right). \tag{2}$$

The value of $\sigma_p$ changes depending on the mission. In the Jason processing, $\sigma_p = 0.513 r_t$ is used, with $r_t$ being the time resolution (3.125 ns). Envisat data have been originally processed with $\sigma_p = 0.53 r_t$ [14]. These are also the values used by ALES for both missions.

In the latest version of the Envisat SGDR, the value of $\sigma_p$ was switched to $0.6567r_t$. As noted in [15], this had a particularly strong impact at low SWH: for real SWH of 1 m, the new values are lower than the previous one by 30 cm and too small compared to that of buoys or models. Moreover, the noise of the retrieval for small waves is now higher, and this is attributed to be a direct consequence of the nonlinear dependence of SWH from $\sigma_p$. In this paper, the effect of the two different values of $\sigma_p$ for Envisat is tested on ALES estimations. In addition using the estimates of $SWH^2$ available in the SGDR product (only for Envisat), an adjusted SGDR SWH field is generated with $\sigma_p = 0.53r_t$ through the following relationship:

$$SWH_{corrected} = \sqrt{SWH^2 + [(0.6567r_t)^2 - (0.53r_t)^2]\,(2c)^2}. \quad (3)$$

ALES performs two estimations for each waveform. The first estimation is performed on the portion of the waveform that goes from the first gates to the end of the leading edge. The SWH obtained from the first step is used to determine the width of the subwaveform to be used in the second estimation, following a linear relationship derived from experiments on simulated data which aims at preserving the precision of the range retrieval at different sea states. The aim of this paper is to assess whether the use of this relationship produces satisfying results also for SWH estimation.

*1) Sampling Issues in Conventional Altimetry:*

*Envisat:* In the standard procedure of pulse-limited altimetry, as a result of the sampling of the individual echo, 128 in-phase/quadrature samples are gathered and fast Fourier transformed (FFT) [3]. For Envisat, the 128 gates of each 18-Hz waveform have been obtained by squaring the modules of the FFT and averaging over 100 echoes. Each of the 128 values of an FFT corresponds to a given frequency. In order to better describe the leading edge, two additional gates have been stored in the SGDR [16]: A discrete Fourier transform (DFT) algorithm was computed on board at two intermediate frequencies chosen to be in the leading edge portion of the waveform, and the corresponding values were then squared and averaged as described earlier in the standard procedure.

The increased sampling also gives a partial solution to the undersampling issue in conventional altimeters, described in [17]. Since the pulse bandwidth of a conventional altimeter is $B = 320$ MHz, to respect the Nyquist theorem, it would be sufficient to sample the signal with a rate corresponding to a gate spacing of $\Delta = c/2B = 0.468$ m, which is the gate spacing of the waveforms. Nevertheless, since both Jason and Envisat form the waveforms by squaring the magnitude of a complex function resulting from the Fourier transformation of the receiver output, the bandwidth is actually doubled, and the waveform is consequently undersampled, due to the fact that the range resolution corresponds to half of the Nyquist rate. This problem is particularly felt in the case of fast rising times (which translated into very low SWH values) since the leading edge of the waveform is poorly described.

The effect of the insertion of the additional gates is tested in ALES together with different values of $\sigma_p$. The results are presented in Section IV-A, and the best method is then used for validation in Section IV-B.

*Jason:* Jason does not provide additional gates, and therefore, in this study, the waveforms are interpolated prior to retracking in order to double the amount of gates by oversampling and increase the redundancy of the information across the leading edge.

An optimal solution would be the interpolation of the complex amplitudes of every single echo before squaring the magnitudes and averaging the results. Individual echoes are not available and therefore this strategy is not feasible. For this study, it was decided to perform on every 20-Hz waveform an Akima interpolation, i.e., a piecewise spline interpolation that fits a smooth curve to the given points [18].

### B. Methods for Validation

The validation is performed by comparing the time series of SWH generated along consecutive satellite passes with the time series generated by buoy measurements in the locations described in Section III. To create an altimetric time series, data points along the satellite tracks need to refer to the same geographical location along track for all cycles. The altimeter data from SGDR and ALES for each cycle were therefore linearly interpolated along the nominal tracks defined by the Centre for Topographic studies of the Ocean and Hydrosphere (CTOH) and available from http://ctoh.legos.obs-mip.fr/altimetry/satellites, neglecting the across-track displacement of different passes along the same track, which is normally less than 1 km.

The difference between ALES and SGDR SWH retrieval and buoy measurements is analyzed in terms of correlation, mean bias, and std at the point nearest to the buoy and at all other points along track. For the along-track correlation analysis, the aim was to determine for each latitude–longitude location the maximum percentage of cycles of data that could be retained while guaranteeing a correlation with the buoy time series of at least 0.9. The test is performed in an iterative way: First of all, for each location, the correlation of the buoy time series with the entire set of altimetry retrievals is checked; if the correlation coefficient is lower than 0.9, then the cycle with the maximum discrepancy (quantified as the maximum of the absolute value of the difference) between the buoy value and altimeter retrieval is excluded. This exclusion is iterated until the correlation rises above 0.9, at which point the percentage of the cycle left assesses the general quality of the retracked altimetry values against the available SGDR product and will be referred to as the percentage of cycles for high correlation (PCHC) throughout the following chapters.

## III. Data

One track from Jason-1 and Jason-2 (J-2 213 and J-1 213) and three tracks from Envisat (Env 543, Env 474, and Env 85) have been reprocessed, and waveforms at 20 Hz for Jason and at 18 Hz for Envisat have been retracked by ALES. The choice of more tracks for Envisat is justified by the different experiments undertaken and the fact that the results were less clear than with Jason. A comparison with data coming from different buoys was therefore necessary and possible owing to the high density of tracks, which was not the case in Jason. On the other side,

TABLE I
DATA SET CHARACTERISTICS. COLUMN 2: BUOY USED FOR VALIDATION. COLUMN 3: MINIMUM DISTANCE BETWEEN THE SATELLITE TRACK AND THE BUOY. COLUMN 4: DISTANCE (OF THE CLOSEST POINT BETWEEN SATELLITE TRACK AND BUOY) FROM THE COAST. COLUMN 5: NUMBER OF CYCLES CONSIDERED IN THE VALIDATION (CYCLES WHERE SATELLITE DATA WERE MISSING AND/OR COINCIDENT BUOY DATA WERE NOT AVAILABLE HAVE BEEN EXCLUDED). COLUMN 6: TIME INTERVAL BETWEEN THE FIRST AND THE LAST CONSIDERED CYCLE IN MONTH–YEAR FORMAT

| | Buoy | Min Distance (km) | Distance from coast (km) | Number of cycles | Time span |
|---|---|---|---|---|---|
| Env 85 | Elbe | 3.2 | 17.3 | 53 | 09-2003 to 09-2010 |
| Env 85 | Helgoland | 16.1 | 8.9 | 48 | 10-2002 to 09-2010 |
| Env 474 | Helgoland | 12.2 | 7.8 | 55 | 12-2002 to 09-2010 |
| Env 474 | Elbe | 11.1 | 16.5 | 62 | 10-2002 to 09-2010 |
| Env 543 | Westerland | 12.3 | 0.3 | 50 | 05-2003 to 10-2010 |
| J1 213 | Helgoland | 10.7 | 9.1 | 141 | 02-2002 to 02-2009 |
| J2 213 | Helgoland | 10.7 | 9.2 | 112 | 07-2008 to 12-2012 |

the high amount of Jason available cycles, owing to the ten-day repetition rate, was a sufficient proof of robustness for the results. *In situ* data come from three buoys which deliver a measurement every 30 min: Helgoland, Elbe, and Westerland. The data are provided by the Bundesamt fuer Seeschiffahrt und Hydrographie (BSH).

Fig. 1 shows the area of study, including the satellite tracks and buoys' locations. It is relevant to point out the flight direction of each satellite as it flies over each region since land-to-sea and sea-to-land transitions might influence the behavior of the on-board tracker (i.e., the algorithm that attempts to keep the received waveform within the radar observation window) in different ways: Env 543, Env 85, and J-2/J-1 213 are ascending tracks (south to north), while Env 474 is descending. The minimum distance between a satellite track and a buoy is 3.2 km, while the maximum distance is 16.5 km. We assume these distances to be acceptable for a meaningful comparison. As a reference, Monaldo [19] estimated a SWH difference of 0.15 to 0.2 m for a separation of 14 km, but this was based on a global data set. The extended stretches of high correlation found in the along-track analysis in Section IV-B2 will, however, serve as a confirmation that our assumption is valid in the coastal region object of this study.

Table I summarizes the characteristics of the data set. For every track, all the cycles for which there was a simultaneous *in situ* measurement (within a 30-min time window) were considered. Monaldo [19] estimated that, when the average temporal separation between the buoy and altimeter is 15 min, the effect in the difference between the two measurements will be about 0.1 m. In order to limit the impact of the temporal separation between the two measurements, the buoy data are resampled in time onto a 1-min grid by means of linear interpolation. Following the resampling, the value closest to the satellite overpass in time is taken as the ground truth.

A peculiarity of the German Bight lies in the variable extension of the dry areas, depending on the tidal phase. This needs to be accounted for to correctly interpret the output of

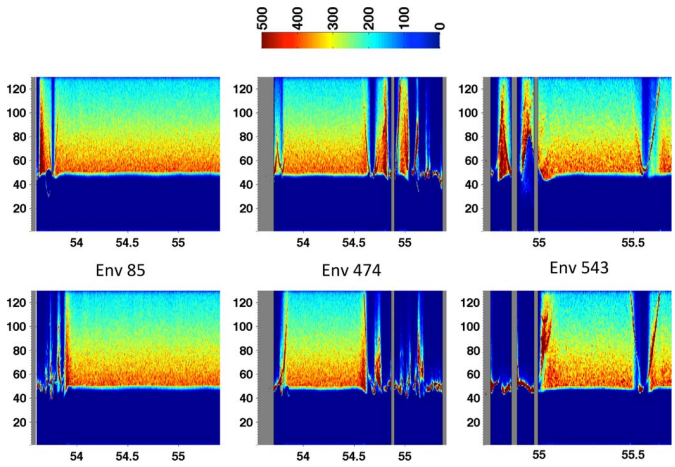


Fig. 2. Two examples of radargrams for each Envisat track: Upper panels correspond to times of high tide, while the lower panels refer to a low-tide situation. Each column corresponds to a high-rate waveform along a satellite track. The horizontal dimension corresponds to the latitude of each waveform. The intensity of the return is color coded from blue to red. The area of the tidal flats is recognizable by the presence of specular waveforms (single narrow peak and no gradual decay in the trailing edge), particularly evident at low tide, when more land lies above the sea level.

the retracking and can be appreciated from the plots (known as radargrams) in Fig. 2. The two radargrams for each of the three considered Envisat tracks show the waveforms for both low- and high-tide events. The $y$-axis corresponds to the gate number, and the $x$-axis corresponds to different waveforms identified by their latitude. ALES is capable to retrack waveforms with a distinct leading edge and a decaying trailing edge, even if corrupted by bright targets. However, particularly in the low-tide phase, waveforms present a single very high spike, which is typical of specular reflections from a flat surface, which could either be land or isolated patches of water. The location of specular returns in the low tide phase can be used as a trace to detect the extension of the tidal flats.

From high-rate waveforms, ALES-retracked SWH is then averaged to generate 1-Hz estimations. A check is performed in order to eliminate outliers on every block of 20 high-rate values $X$: the median value and the scaled median absolute deviation ($\widehat{MAD}$) are computed. Each estimation $x$ is considered valid if

$$x < median(X) + 3 \times \widehat{MAD}(X)$$

or

$$x > median(X) - 3 \times \widehat{MAD}(X)$$

where

$$\widehat{MAD}(X) = 1.4286 \times median\left(|X - median(X)|\right).$$

The $\widehat{MAD}$ scaled using the factor 1.4286 is approximately equal to the std for a normal distribution. Statistics based on the median are more robust and suitable for outlier detection and have been already applied to satellite data [20]. Once the outliers have been excluded, the median of the remaining points is computed in order to generate the 1-Hz estimation.

The SWH estimations for Jason were corrected using the instrumental corrections described in [21] and [22].

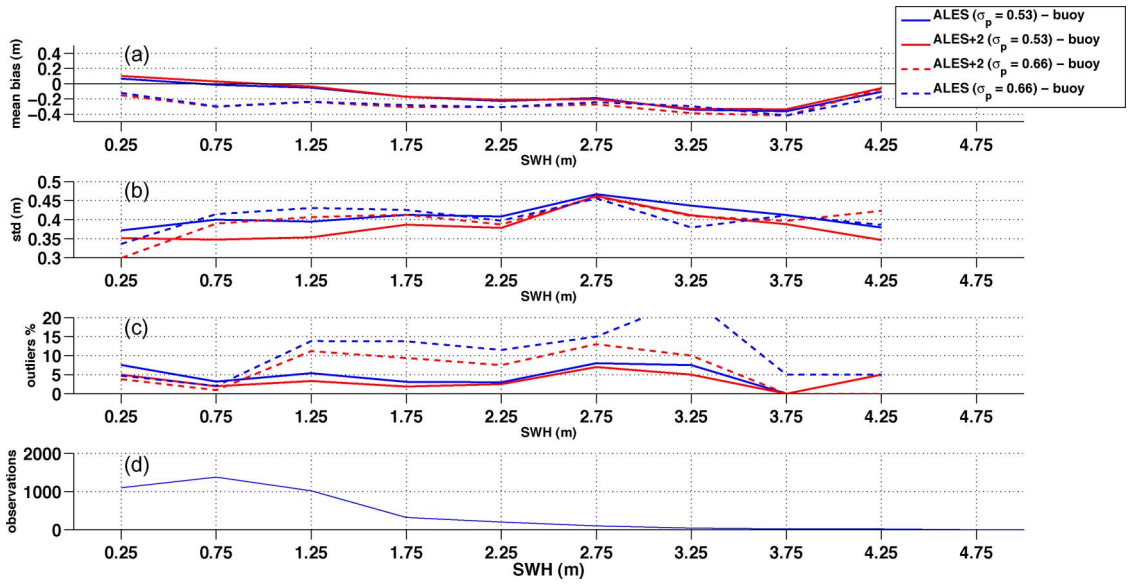


Fig. 3. Analysis of four different retracking strategies for Envisat. Statistics are produced considering the 20 nominal high-rate points from Env 474 and Env 85 closest to the Helgoland buoy and the high-rate points from Env 85 closest to the Elbe buoy. The difference between ALES SWH retrieval and buoy measurements is analyzed in terms of (a) mean bias, (b) std, (c) percentage of outliers, and (d) number of available observations for varying SWH.

## IV. Results and Discussion

### A. Choice of the Retracking Strategy for Envisat

For Envisat, to evaluate both the effect of different $\sigma_p$ values and of the additional DFT gates, we consider the 20 nominal high-rate locations closest to each buoy. The points along Env 543 close to the Westerland buoy, which is located at 0.3 km from the coast (see Table I), are not included in this analysis due to the inaccuracy of the corresponding altimetry estimates.

The difference between the ALES SWH retrieval and the *in situ* data is analyzed in terms of mean bias and std for different values of SWH. When the modulus of the difference is bigger than 1 m, the measurement is considered to be an outlier and is not included in the computation of bias and std. The results of the analysis are displayed in Fig. 3. Results are shown for varying SWH at intervals of 50 cm, i.e., the 0.25-m point on the $x$-axis includes all the data for which the corresponding *in situ* SWH estimations are between 0 and 50 cm. Panel D shows the number of available observations for varying SWH. Most of the observations are at low sea states (SWH $< 2.5$ m), and only very few measurements are available for more extreme situations. This limits the validity of our study to low sea states, which are nevertheless considered particularly challenging to be detected by retracking algorithms, since a sharp leading edge in a waveform is described by fewer gates and, therefore, the derived estimate of the rising time is percentually less accurate.

Concerning the choice of $\sigma_p$, panel A shows that a higher $\sigma_p$ produces a lower SWH estimation (roughly 20 cm of difference for the low sea state). Compared to *in situ* data, the higher $\sigma_p$ leads to a marked underestimation. Similar conclusions were found in [15].

Looking at the addition of the two DFT intermediate gates (referred to as ALES+2 in the figure), we see from the std (panel B) that this strategy has a positive effect in terms of noise reduction. Moreover, for SWH smaller than 0.5 m, a lower std is shown for the estimations that adopt the $\sigma_p = 0.6567 r_t$. This is due to the fact that several estimations of $\sigma_c$ are smaller than $\sigma_p$ and therefore show up as zeros in the SWH value. Setting $SWH = 0$ for every negative value of $SWH^2$ is a practice adopted in the current versions of the official products. If, on one side, it generates anomalous low std values, it must also be said that, given that a negative SWH cannot be a physically plausible sea state, a null SWH represents the closest realistic estimation. Using $\sigma_p = 0.53 r_t$ significantly reduces the null estimations, and therefore, the statistics show a much more realistic std value.

Overall, ALES+2 with $\sigma_p = 0.53$ is the retracking scheme with the best performances, including the smallest percentage of estimations which have more than 1 m of difference with the ground truth (indicated as outliers in panel C).

Although this paper is focused on SWH retrieval, it is important to note that the insertion of the two DFT gates does not change significantly the range estimation. Experiments carried out along Env 85 in the open sea interval between 54.4° and 55.2° of latitude showed that the range estimations with and without the two DFT gates are 99.97% correlated, with a 2-mm bias and a 1-mm std.

### B. Validation

*1) Analysis at the Closest Locations:* The first stage of the validation against *in situ* data is the analysis at the closest point between the buoys and the corresponding satellite tracks. Fig. 4 shows the results for the three Envisat tracks, with the upper two plots showing the comparison of Env 85 with two buoys at the respective closest points. Each circle (red for ALES and blue for SGDR) shows the retracked SWH value corresponding to the ground truth (on the $x$-axis) at a specific cycle. The SWH from Envisat adjusted by using $\sigma_p = 0.53 r_t$ is shown in black squares. In the same way, Fig. 5 shows the results for pass 213 from Jason-2 (plots on the left) and Jason-1 (plots on the right). For Jason, the analysis is performed for high-rate estimations (upper plots) and 1-Hz points (lower plots).

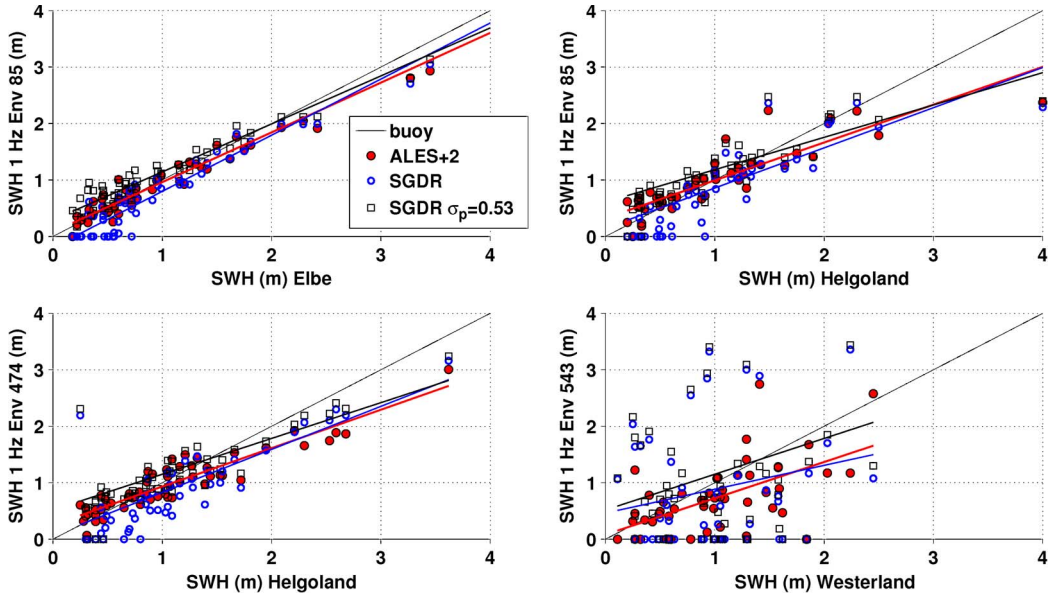


Fig. 4. Scatterplot of Envisat-retracked SWH against the corresponding *in situ* estimations at the closest 1-Hz point of the satellite track to the buoy. Shown are the results with (full circle) ALES with waveforms augmented by two gates, (open circle) standard SGDR, and (open square) SGDR recomputed using a different $\sigma_p$.

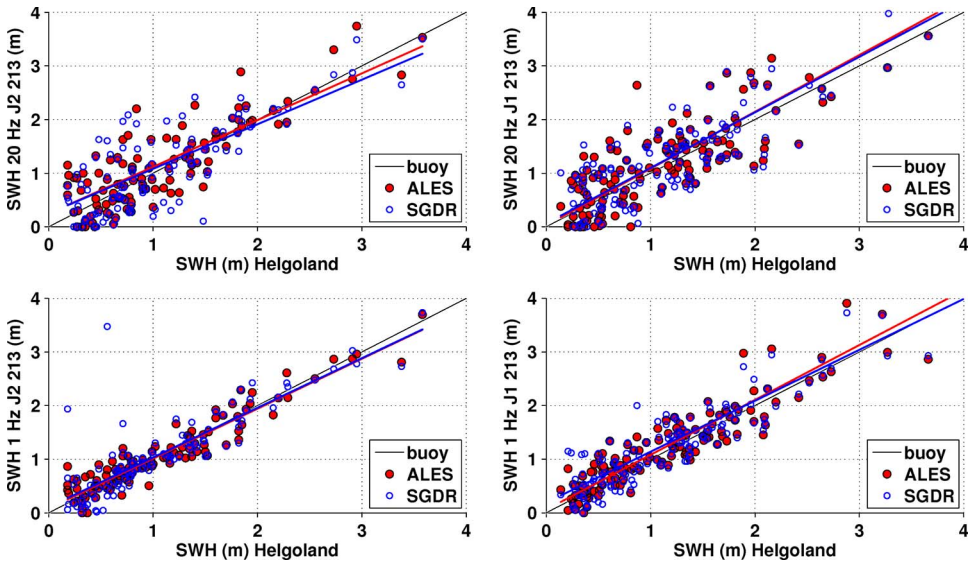


Fig. 5. Scatterplot of Jason retracked SWH against the corresponding *in situ* estimations at the closest point of the satellite track to the buoy. The upper plots refer to the 20-Hz data, and the lower plots refer to the 1-Hz data. The plots on the left refer to Jason-2, and the plots on the right refer to Jason-1. Shown are the results with (full circle) ALES and (open circle) standard SGDR.

The straight lines are the best fit of the data. A summary of the results in terms of correlation coefficient, slope, bias, and std w.r.t. the buoy estimations is reported in Table II for Envisat and in Table III for Jason. All the points are considered, and no outliers are removed, in order to give the best possible evaluation of the available data set. For Envisat, statistics for SGDR adjusted with $\sigma_p = 0.53 r_t$ are shown in brackets. For space reasons, only one "double comparison" of the same track with two buoys is shown in the plots (Envisat 85 against the Helgoland and the Elbe buoy), while the comparison of Envisat 474 with the Elbe buoy is reported only in the table.

*Envisat:* For the Envisat tracks, the analysis is performed on the 1-Hz data since high-rate SWH is not available in the SGDR. The point of Env 543 closest to the Westerland buoy presents particularly bad estimations for both SGDR and ALES data sets. As previously mentioned, the reason is that the point is located at a distance of only 0.3 km from the coast. At this distance, there is often no clear leading edge in the waveforms, and therefore, even a subwaveform application of the Brown model is often inadequate. It is anyway relevant that ALES estimations are much closer to the ground truth than SGDR.

Considering all the tracks, the underestimation of SGDR is evident, with several estimations being zeros, due to the fact that SGDR uses $\sigma_p = 0.6567 r_t$. This underestimation, assessed as the median bias, is never less than 20 cm, except for Envisat 474 compared to the Elbe buoy. The median bias of ALES is less than 10 cm for all the comparisons. The use of $\sigma_p = 0.53 r_t$ in the SGDR product brings to an improvement in terms of bias in four out of five comparisons, although the low wave heights are overestimated. The slopes suggest for both the data

TABLE II
VALIDATION RESULTS OF THE NOMINAL SATELLITE TRACKS (FOR ENVISAT) AT THE 1-HZ POINTS CLOSEST TO EACH BUOY, IN TERMS OF THE FOLLOWING: (COLUMN 3) CORRELATION, (COLUMN 4) SLOPE OF THE LINEAR FIT, (COLUMN 5) MEDIAN BIAS COMPUTED SUBTRACTING EACH BUOY ESTIMATION FROM THE CORRESPONDING RETRACKED SWH, AND (COLUMN 6) STD W.R.T. THE BUOY ESTIMATIONS. STATISTICS FOR SGDR ADJUSTED WITH $\sigma_p = 0.53 r_t$ ARE SHOWN IN BRACKETS. THE BUOY OF REFERENCE IS REPORTED IN BRACKETS IN THE FIRST COLUMN

| | | Correlation | Slope | Bias (m) | StD (m) |
|---|---|---|---|---|---|
| Env 85 (Helgoland) | SGDR | 0.56 (0.52) | 0.71 (0.57) | -0.23 (0.12) | 0.69 (0.69) |
| | ALES | 0.89 | 0.63 | 0.09 | 0.27 |
| Env 85 (Elbe) | SGDR | 0.97 (0.97) | 0.99 (0.85) | -0.22 (0.13) | 0.18 (0.15) |
| | ALES | 0.97 | 0.88 | -0.01 | 0.13 |
| Env 474 (Helgoland) | SGDR | 0.63 (0.60) | 0.76 (0.63) | -0.31 (0.05) | 0.56 (0.58) |
| | ALES | 0.93 | 0.65 | 0.00 | 0.20 |
| Env 474 (Elbe) | SGDR | 0.91 (0.90) | 1.06 (0.90) | -0.05 (0.23) | 0.21 (0.22) |
| | ALES | 0.97 | 0.97 | 0.09 | 0.08 |
| Env 543 (Westerland) | SGDR | 0.20 (0.15) | 0.42 (0.63) | -0.48 (0.16) | 0.67 (0.58) |
| | ALES | 0.55 | 0.55 | -0.01 | 0.41 |

TABLE III
VALIDATION RESULTS OF THE NOMINAL SATELLITE TRACKS (FOR JASON) AT THE POINTS CLOSEST TO EACH BUOY, IN TERMS OF THE FOLLOWING: (COLUMN 3) CORRELATION, (COLUMN 4) SLOPE OF THE LINEAR FIT, (COLUMN 5) MEDIAN BIAS COMPUTED SUBTRACTING EACH BUOY ESTIMATION FROM THE CORRESPONDING RETRACKED SWH, AND (COLUMN 6) STD W.R.T. THE BUOY ESTIMATIONS. THE BUOY OF REFERENCE IS REPORTED IN BRACKETS IN THE FIRST COLUMN

| | | Correlation | Slope | Bias (m) | StD (m) |
|---|---|---|---|---|---|
| J2 213 - 1 Hz (Helgoland) | SGDR | 0.85 | 0.93 | - 0.04 | 0.34 |
| | ALES | 0.95 | 0.90 | -0.01 | 0.15 |
| J2 213 - 20 Hz (Helgoland) | SGDR | 0.80 | 0.83 | 0.07 | 0.67 |
| | ALES | 0.85 | 0.87 | 0.01 | 0.57 |
| J1 213 - 1 Hz (Helgoland) | SGDR | 0.81 | 0.95 | 0.03 | 0.52 |
| | ALES | 0.93 | 0.98 | 0.11 | 0.23 |
| J1 213 - 20 Hz (Helgoland) | SGDR | 0.86 | 1.04 | -0.02 | 0.55 |
| | ALES | 0.87 | 1.06 | -0.01 | 0.33 |

sets a progressive underestimation of SWH as the values of the buoy increase, but the number of observations at SWH $> 2$ m is too small to draw a conclusion. All the statistics show a marked improvement in ALES. This is particularly true in the comparisons with the Helgoland buoy (correlation increases by $\sim$0.3, and std halves). This is expected since the calm coastal waters and the land of Helgoland islands produce bright targets visible in the radargrams, which corrupt the leading edge and have consequences on the estimations of the standard product.

*Jason:* The statistics obtained from the ALES-retracked data set show significant improvements in all terms compared to the corresponding SGDR product. The most significant improvement concerns the std of the differences between altimetry estimations and buoy values, which leads to a variance reduction by a factor of 5 at 1 Hz. Compared to Envisat, the slopes of the fitted straight lines are more correct since the values of SWH higher than 2 m are not underestimated. As in Envisat though, statistics are much more robust for lower SWH. No systematic bias is present, which means that the $\sigma_p$ value in use (which, in this case, is the same both in ALES and in SGDR) is appropriate.

*2) Along-Track Analysis:* Along-track performances in terms of correlation at 20 Hz (18 Hz) and 1 Hz and median values of the std and the bias at 1 Hz considering all the available cycles (all w.r.t. the buoy estimations) were computed for ALES- and SGDR-retrieved SWH. The results are shown in Fig. 6 for Env 85 against the Helgoland and the Elbe buoys, Fig. 7 for Env 474 against the Helgoland buoy and Env 543 against the Westerland buoy, and Fig. 8 for J1 213 and J2 213 against the Helgoland buoy.

*Envisat:* Considering the PCHC (see Section II-B for the methodology), it is evident that, in the open sea, the steps followed to derive the 1-Hz estimations from the high-rate values and described in Section III improve the correlation. It is also noticeable that the wave height signal is well correlated along the entire considered length of the satellite tracks (except close to the tidal flats), which suggests that the SWH field in the area is dominated by synoptic scales and confirms the validity of our assumption that a comparison between altimeter and buoys is meaningful despite the spatial separation. Looking at the same track (Env 85) compared to two different buoys (Helgoland and Elbe) reveals that high-rate estimations are more correlated with Elbe than with Helgoland *in situ* data. This can be related to the position of the Helgoland buoy, which is located at 2 km of distance from an island, and therefore, the local sea state can also be influenced by small scale phenomena such as changes of wind patterns due to the sheltering caused by the land. The presence of the Helgoland island itself influences the high-rate data due to specular reflections that alter the standard shape of an oceanic waveform as explained in the previous section: This has an impact on the correlation, which is visible along tracks Env 85 and Env 474 for the latitude interval of 54.1°–54.3°. It also leads to a lower PCHC for the 1-Hz points in the same area for the SGDR, while ALES data succeed in keeping more cycles to obtain the same level of correlation.

The areas of the tidal flats show drastic drops in PCHC. ALES 18-Hz estimations generally present a PCHC between 20% and 40% in these areas. Nevertheless, the values averaged at 1 Hz have a lower percentage, which is sometimes overtaken by the original SGDR 1-Hz product. It must be noticed that, even at high tide, the sea state in the tidal flats will be heavily influenced by the shallow water, and therefore, the correlation of the signal with an offshore buoy is likely to be less significant. In the tidal flats, since the 1-Hz points for ALES have a lower PCHC than the corresponding 18-Hz estimations, it might be worth to perform a more careful screening of the data set, for example, considering the estimated sea level, the backscatter coefficient, and the goodness of waveform fit to avoid considering wrong estimations. This is not done in this study, which is focused on the quality of the raw data.

Considering the median of the stds at 1 Hz, ALES succeeds in keeping it below 0.5 m all along the track in the open sea, showing a constant improvement if compared to the SGDR product.

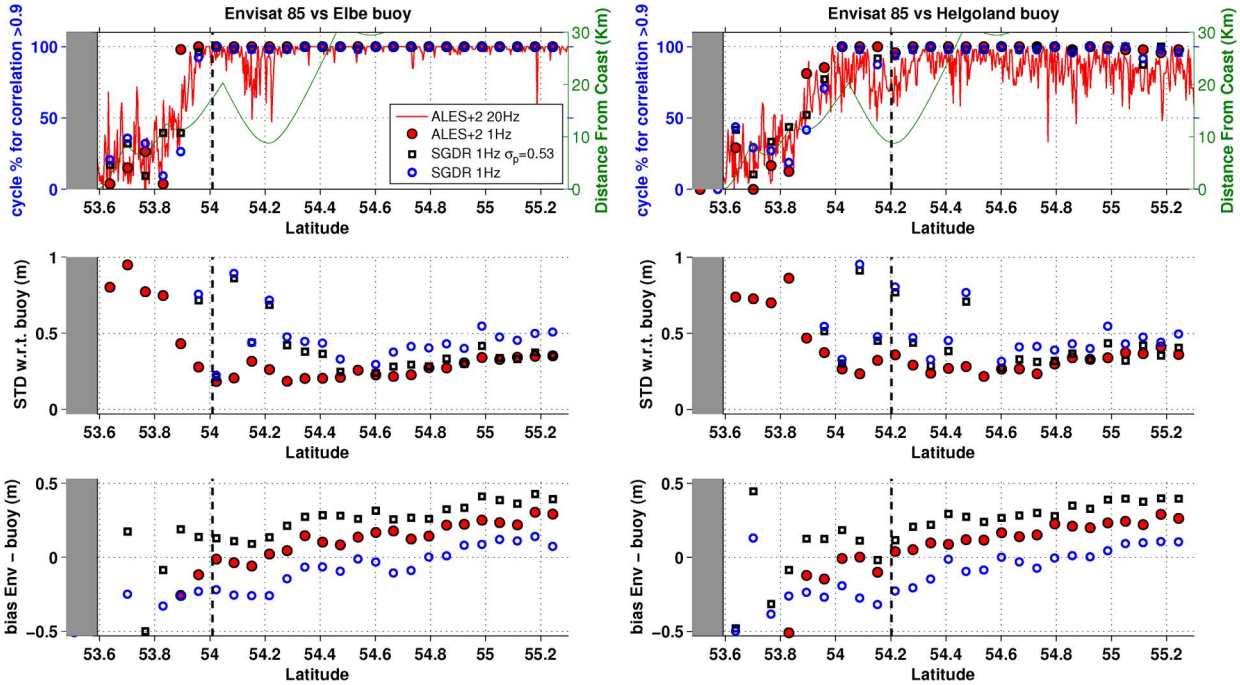


Fig. 6. Along-track validation of SWH estimations for Envisat pass 85 against data from (left) Elbe and (right) Helgoland buoys in terms of (top) PCHC at 1 and 18 Hz, (center) std of 1-Hz estimations from buoy values, and (bottom) median bias of 1-Hz estimations. On the $x$-axis, the along-track latitude of the nominal tracks is shown. Land is shaded in gray. The closest point of the track from the buoy is highlighted by a black dashed vertical line. The distance up to 30 km from the closest coastline is specified by a green line which refers to the $y$-axis on the right.

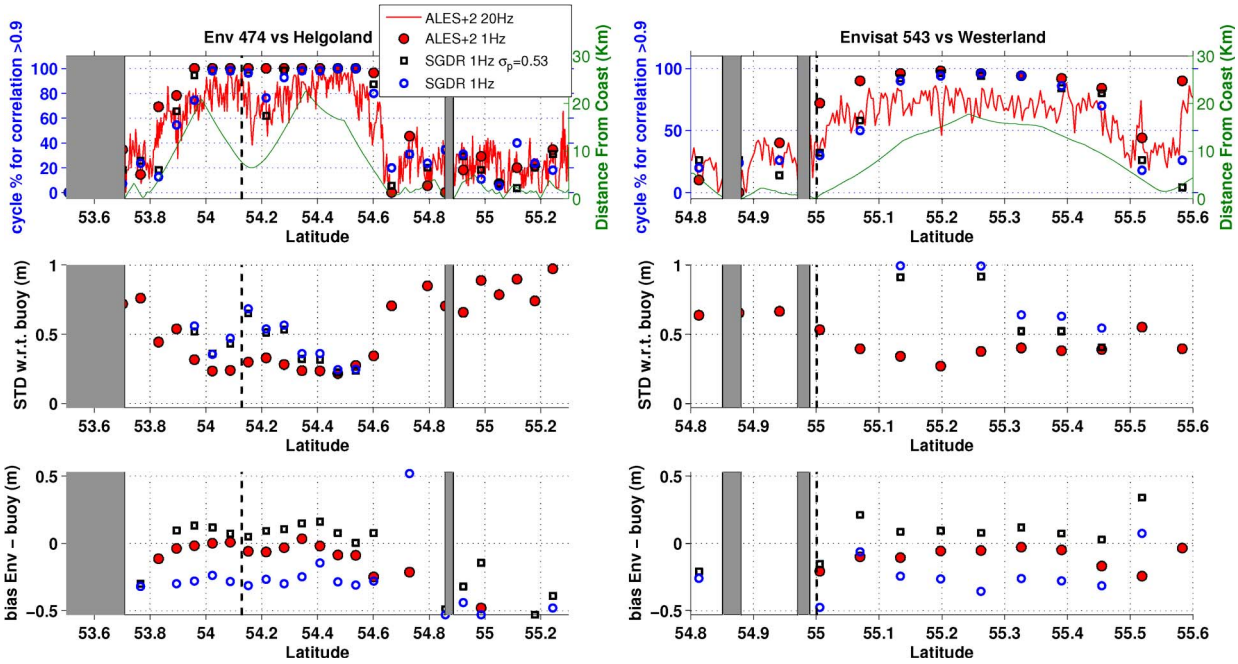


Fig. 7. Along-track validation of SWH estimations for (left) Envisat pass 474 against data from the Helgoland buoy and (right) Envisat pass 543 against data from the Westerland buoy in terms of (top) PCHC at 1 and 18 Hz, (center) std of 1-Hz estimations from buoy values, and (bottom) median bias of 1-Hz estimations. On the $x$-axis, the along-track latitude of the nominal tracks is shown. Land is shaded in gray. The closest point of the track from the buoy is highlighted by a black dashed vertical line. The distance up to 30 km from the closest coastline is specified by a green line which refers to the $y$-axis on the right.

The bias of ALES for Env 85 and Env 474 reaches its minimum at the point closest to the buoy, as expected, while SGDR is constantly biased of about 20 to 30 cm all along the tracks. The SGDR product modified as shown in (3) overestimates the SWH compared to the ground truth and to the ALES estimates, despite the same $\sigma_p$ approximation adopted. This suggests that the best value of $\sigma_p$ can be different for different retracking algorithms and that the original $\sigma_p$ approximation used in the previous SGDR version brings the best result when applied to a subwaveform retracker such as ALES.

Generally, for all the tracks, the PCHC has a decay steeper in SGDR than in ALES when approaching the coast. It is therefore inferred from the plots that ALES is able to retrieve an unbiased estimation of SWH also when the trailing edge of

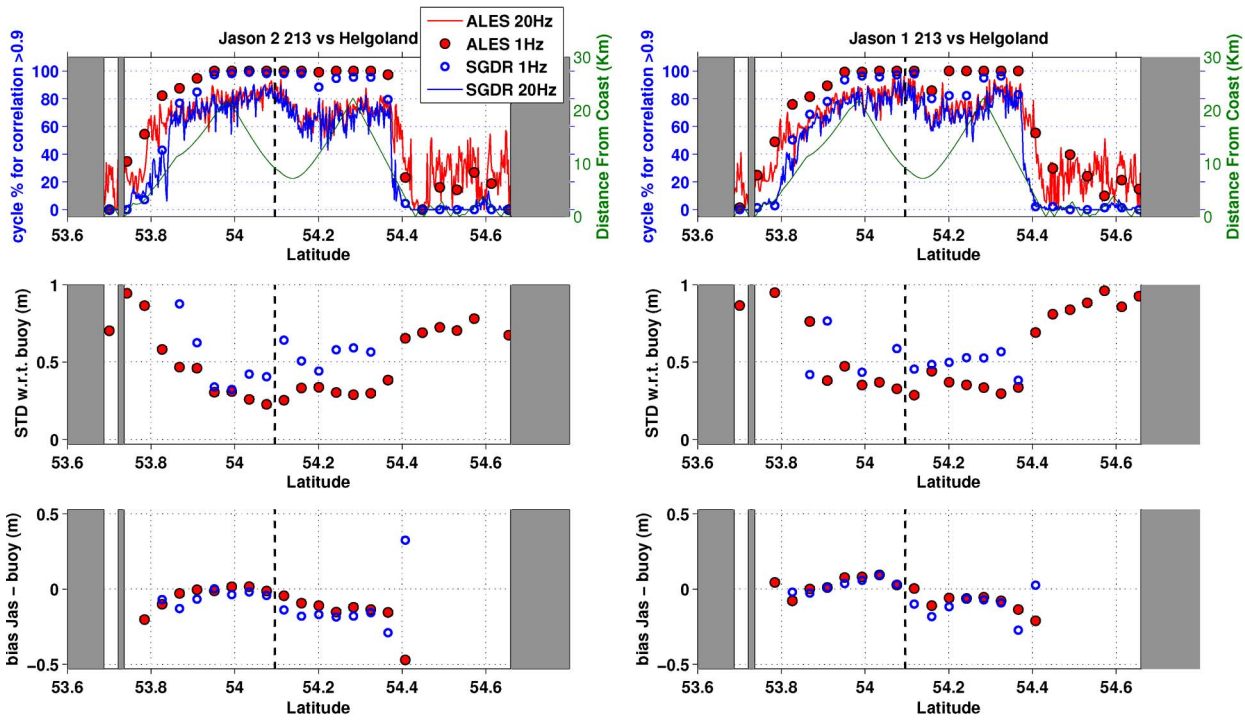


Fig. 8. Along-track validation of SWH estimations for (left) Jason-2 and (right) Jason-1 pass 213 against data from the Helgoland buoy in terms of (top) PCHC at 1 and 20 Hz, (center) std of 1-Hz estimations from buoy values, and (bottom) median bias of 1-Hz estimations. On the $x$-axis, the along-track latitude of the nominal tracks is shown. Land is shaded in gray. The closest point of the track from the buoy is highlighted by a black dashed vertical line. The distance up to 30 km from the closest coastline is specified by a green line which refers to the $y$-axis on the right.

an oceanic waveform is corrupted by highly reflective targets and to increase the amount of good estimations in the coastal region close to the tidal flats.

*Jason:* The comparison with Jason SGDR in terms of PCHC with the buoy estimations is even more reliable than the corresponding one with Envisat data since 20-Hz SGDR estimations of SWH are available (unlike in Envisat) and since each track has a higher number of cycles. ALES improves the quality of SWH estimations and is constantly more correlated than the original SGDR product. Not only does it show improvements when the satellite track is close to the tidal flat area, but it also succeeds in having a PCHC between 20% and 40% in the tidal flats, where very few estimations from the SGDR are available. In terms of std w.r.t. the buoy estimation, there is a marked improvement brought by the ALES product, which keeps the values below 0.5 m until the tidal flats, with a slight improvement when considering Jason-2 compared to Jason-1. The improvements in Jason-2 are probably due to the smaller mispointing values compared to Jason-1, which improves the accuracy in the estimates of rise time of the leading edge and amplitude.

The results obtained in terms of bias are satisfactory, despite the fact that Jason-1 corrections mentioned in Section III are derived for a four-parameter retracking algorithm (the off-nadir angle is added as an unknown value to be estimated in the Brown functional form) while ALES performs a three-parameter estimation. From the along-track analysis, there is no significant systematic bias between SGDR data and buoy estimations. This is attributable to the fact that the same $\sigma_p$ approximation was used in SGDR and ALES, as opposed to what has been seen in the previous section for Envisat. It must be noted that the results in terms of bias and std for SGDR over the tidal flats are not significant, as less than 5% of the cycles contain an estimated SGDR value in those locations.

## V. Conclusion

The present study aims at validating the SWH estimated by the ALES satellite altimetry retracker against *in situ* buoys located in the German Bight. One of the main objective is to assess the improvements brought by a coastal dedicated retracking scheme compared to standard products released for three different satellite altimetry missions. Despite the fact that this is a local validation exercise, the use of multiple buoys and multiple tracks in the case of Envisat and the high number of cycles and the clear results in the case of Jason make a case for a more general extension of the conclusions. Nevertheless, the robustness of the findings is limited to low SWH ($< 2.5$ m); this, however, includes conditions considered particularly challenging in altimetry, due to poor leading edge sampling.

We have shown that ALES is able to extend the quality and the quantity of SWH retrievals toward the coast while remaining highly reliable in the open sea as well. An improvement is seen in terms of PCHC for one to three 1-Hz points toward the coast for each of the tracks (for both Envisat and Jason missions), meaning about 7 to 22 km in terms of spatial improvement. A typical example of ALES improved SWH estimations is found for the Envisat track 543, which runs almost parallel to the coastline and where the entire retracked area lies closer than 20 km from the coast: ALES estimations are constantly better than the SGDR data set, considering all the statistics. As expected, ALES is able to correctly retrieve SWH

in areas where the presence of highly reflective bright targets in the satellite footprint corrupts the trailing edge of the waveform.

In the tidal flat area, which extends much further from the coastline and includes land that is submerged or exposed depending on the tidal phase, several well correlated cycles are retrievable: For Jason, the improvement brought by ALES is clear because the standard SGDR product fails to give any estimation in the vast majority of cases; for Envisat, results are less obvious due to the high amount of specular returns, which differ substantially from the Brown model adopted by ALES and are not always retracked correctly by the algorithm. Further research is needed to establish whether the signal coming from these areas can be correlated with the data from offshore buoys, given that the sea state will be highly influenced by the very low depth, and to relate more carefully the tidal phase with the sea level all over the area and the consequent returned echo in the altimetry signal.

Not only ALES estimations are reliable both in the coastal area and in the open sea, but also the 1-Hz estimations have a constantly lower std compared to the original SGDR product. Further research is needed in selecting the best high-rate estimations before averaging to 1 Hz, to provide an enhancement of the capabilities also in the more challenging area of the tidal flats.

A widespread underestimation of low SWH is found in the latest version of the Envisat SGDR product, and the cause is the value used to approximate the width of the PTR function in the Brown functional form for the SGDR retracking. Our analysis suggests that the previous value of $\sigma_p = 0.53r_t$ (with $r_t$ being the time resolution) is a better one, although when applied to SGDR, it brings the opposite problem of an overestimation of low SWH resulting from an overestimation of the rise time, probably due to the presence of spikes in the waveform tail, which is not seen in ALES estimates. The new ALES retracking strategy makes use of the two additional DFT gates provided in the SGDR: It is found that the increased leading edge sampling reduces the std w.r.t. the ground truth from *in situ* data and increases the amount of correct estimations, while the corresponding range estimates are not significantly different from the ones derived from the original waveforms.

This research shows how the adoption of ALES retracking strategy can improve the current SWH data set in the coastal seas, which could give a significant help to describe the sea state and the interactions with wind forcing in coastal areas where no buoys are located. This has promising implications in view of using reprocessed coastal altimetry data for the validation of wave models and wave data retrieved from other remote sensing instruments.

## ACKNOWLEDGMENT

The authors acknowledge the kind support from the German Waterway and Shipping Administration (WSV) and the Federal Maritime and Hydrographic Agency (BSH) for the *in situ* data and European Space Agency (ESA) and National Oceanic and Atmospheric Administration (NOAA) for the altimeter data. The authors would like to thank G. Quartly, W. Smith, and C. Buchhaupt for their suggestions and genuine interest.

## REFERENCES

[1] I. Young, "Seasonal variability of the global ocean wind and wave climate," *Int. J. Climatol.*, vol. 19, no. 9, pp. 931–950, Jul. 1999.
[2] S. Lehner, A. Pleskachevsky, and M. Bruck, "High-resolution satellite measurements of coastal wind field and sea state," *Int. J. Remote Sens.*, vol. 33, no. 23, pp. 7337–7360, Dec. 2012.
[3] D. B. Chelton, J. C. Ries, B. J. Haines, L.-L. Fu, and P. S. Callahan, "Satellite altimetry," in *Satellite Altimetry and Earth Sciences: A Handbook of Techniques and Applications*, vol. 69, L.-L. Fu and A. Cazenave, Eds. San Diego, CA, USA: Academic, 2001.
[4] J.-G. Li and M. Holt, "Validation of a regional wave model with Envisat and buoy observations," in *Proc. Envisat Symp.*, 2007, pp. 23–27.
[5] V. Bhatt, R. Kumar, S. Basu, and V. K. Agarwal, "Assimilation of altimeter significant wave height into a third-generation global spectral wave model," *IEEE Trans. Geosci. Remote Sens.*, vol. 43, no. 1, pp. 110–117, Jan. 2005.
[6] G. D. Quartly, M. A. Srokosz, and A. C. McMillan, "Analyzing altimeter artifacts: Statistical properties of ocean waveforms," *J. Atmos. Ocean. Technol.*, vol. 18, no. 12, pp. 2074–2091, Dec. 2001.
[7] G. Brown, "The average impulse response of a rough surface and its applications," *IEEE Trans. Antennas Propag.*, vol. AP-25, no. 1, pp. 67–74, Jan. 1977.
[8] G. S. Hayne, "Radar altimeter mean return waveforms from near-normal-incidence ocean surface scattering," *IEEE Trans. Antennas Propag.*, vol. AP-28, no. 5, pp. 687–692, Sep. 1980.
[9] J. Gomez-Enri *et al.*, "Modeling ENVISAT RA-2 waveforms in the coastal zone: Case study of calm water contamination," *IEEE Trans. Geosci. Remote Sens.*, vol. 7, no. 3, pp. 474–478, Jul. 2010.
[10] M. Passaro, P. Cipollini, S. Vignudelli, G. Quartly, and H. Snaith, "ALES: A multi-mission subwaveform retracker for coastal and open ocean altimetry," *Remote Sens. Environ.*, vol. 145, pp. 173–189, Apr. 2014.
[11] K. Mittendorf, M. Kohlmeier, and W. Zielke, "A hind-cast data base for the design of offshore wind energy structures in the German Bight," in *Proc. Coast. Eng. Conf.*, 2004, vol. 29, no. 1, p. 740.
[12] L. Fenoglio-Marc *et al.*, "The German Bight: A validation of Cryosat-2 altimeter data in SAR mode," *Adv. Space Res.*, submitted for publication.
[13] J. Schulz-Stellenfleth and E. Stanev, "Statistical assessment of ocean observing networks—A study of water level measurements in the German Bight," *Ocean Model.*, vol. 33, no. 3/4, pp. 270–282, 2010.
[14] C. Gommenginger *et al.*, "Retracking altimeter waveforms near the coasts," in *Coastal Altimetry*, S. Vignudelli, A. Kostianoy, P. Cipollini, and J. Benveniste, Eds. Berlin, Germany: Springer-Verlag, 2011, pp. 61–102.
[15] A. Ollivier and M. Guibbaud, "Envisat RA2/MWR reprocessing impact on ocean data," Collecte Localisation Satell., Ramonville-St-Agne, France, ESA CLS.DOS/NT/12.064, 2012.
[16] B. Soussi and P. Femenias, *ENVISAT RA-2/MWR Level 2 User Manual.* Paris, France: ESA, 2006, ser. ESA User Manual.
[17] J. R. Jensen, "Radar altimeter gate tracking: Theory and extension," *IEEE Trans. Geosci. Remote Sens.*, vol. 37, no. 2, pp. 651–658, Mar. 1999.
[18] H. Akima, "A new method of interpolation and smooth curve fitting based on local procedures," *J. ACM*, vol. 17, no. 4, pp. 589–602, Oct. 1970.
[19] F. Monaldo, "Expected differences between buoy and radar altimeter estimates of wind speed and significant wave height and their implications on buoy-altimeter comparisons," *J. Geophys. Res., Oceans*, vol. 93, no. C3, pp. 2285–2302, Mar. 1988.
[20] A. Alvera-Azcárate, D. Sirjacobs, A. Barth, and J.-M. Beckers, "Outlier detection in satellite data using spatial coherence," *Remote Sens. Environ.*, vol. 119, pp. 84–91, Apr. 2012.
[21] P. Thibaut *et al.*, "Jason-1 altimeter ground processing look-up correction tables," *Mar. Geod.*, vol. 27, no. 3/4, pp. 409–431, Jul. 2004.
[22] P. Thibaut, J. Poisson, E. Bronner, and N. Picot, "Relative performance of the MLE3 and MLE4 retracking algorithms on Jason-2 altimeter waveforms," *Mar. Geod.*, vol. 33, no. S1, pp. 317–335, Aug. 2010.

**Marcello Passaro** (S'14) received the B.S. degree in aerospace engineering from the Politecnico di Milano, Milan, Italy, in 2007 and the M.Sc. degree in Earth-oriented space science and technology from the Technische Universitaet Muenchen, Munich, Germany, in 2009. He is currently working toward the Ph.D. degree at the Graduate School of the National Oceanography Centre, Southampton, U.K., and he is also a trainee at the European Space Agency European Space Research Institute (ESRIN) in Frascati, Italy. His research is focused on satellite oceanography and its application to climate change studies.

**Luciana Fenoglio-Marc** (M'14) received the laurea degree in mathematics (M.Sc.) from the University of Turin, Torino, Italy, and the Ph.D. degree in geodesy from the University of Darmstadt, Darmstadt, Germany, in 1996.

She is currently with the University of Darmstadt in the Institute of Geodesy, Department of Physical and Satellite Geodesy of the Faculty of Civil and Environmental Engineering. Her main research interests are the applications of space techniques to sea level and climate change. She has been involved in studies and projects aiming at improving and validating the altimeter mission data in the coastal zone. She is a Principal Investigator for CryoSat-2 and Saral/AltiKa and is member of the Sentinel-3 Validation Team.

**Paolo Cipollini** (S'93–M'97–SM'03) received the laurea (M.Eng.) degree in electronics engineering from the University of Pisa, Pisa, Italy, in 1992 and the Ph.D. degree in methods and technologies for environmental monitoring from the University of Florence, Firenze, Italy, in 1996.

He is an engineer and satellite oceanographer at the National Oceanography Centre, Southampton, U.K., working on R&D in satellite radar altimetry and its application to remote sensing of the oceans and the coastal zone. He was the overall manager of the ESA development of COASTalt ALTimetry (COASTALT) project (2008–2012) for the development of coastal altimetry for Envisat and is a member of the Ocean Surface Topography Science Team and a Principal Investigator in Cryosat-2 and and Sentinel-3 projects.